applied sciences

MDPI

Article

Effect of Working Atmospheres on the Detection of Diacetyl by Resistive SnO_2 Sensor

Andrea Gnisci [1,*], Antonio Fotia [2], Lucio Bonaccorsi [3] and Andrea Donato [3]

[1] Department of Heritage, Architecture, Urbanism (PAU), University Mediterranea of Reggio Calabria, Via dell'Università 25, 89124 Reggio Calabria, Italy
[2] Department of Information Engineering, Infrastructures and Sustainable Energy, University Mediterranea of Reggio Calabria, Via Graziella Loc. Feo di Vito, 89124 Reggio Calabria, Italy; antonio.fotia@unirc.it
[3] Department of Civil, Energy, Environment and Material Engineering, University Mediterranea of Reggio Calabria, Via Graziella Loc. Feo di Vito, 89124 Reggio Calabria, Italy; lucio.bonaccorsi@unirc.it (L.B.); andrea.donato@unirc.it (A.D.)
* Correspondence: andrea.gnisci@unirc.it

Abstract: Nanostructured metal oxide semiconductors (MOS) are considered proper candidates to develop low cost and real-time resistive sensors able to detect volatile organic compounds (VOCs), e.g., diacetyl. Small quantities of diacetyl are generally produced during the fermentation and storage of many foods and beverages, conferring a typically butter-like aroma. Since high diacetyl concentrations are undesired, its monitoring is fundamental to identify and characterize the quality of products. In this work, a tin oxide sensor (SnO_2) is used to detect gaseous diacetyl. The effect of different working atmospheres (air, N_2 and CO_2), as well as the contemporary presence of ethanol vapors, used to reproduce the typical alcoholic fermentation environment, are evaluated. SnO_2 sensor is able to detect diacetyl in all the analyzed conditions, even when an anaerobic environment is considered, showing a detection limit lower than 0.01 mg/L and response/recovery times constantly less than 50 s.

Keywords: nanomaterials; MOS; resistive sensor; tin oxide; fermentation; diacetyl

Citation: Gnisci, A.; Fotia, A.; Bonaccorsi, L.; Donato, A. Effect of Working Atmospheres on the Detection of Diacetyl by Resistive SnO_2 Sensor. *Appl. Sci.* **2022**, *12*, 367. https://doi.org/10.3390/app12010367

Academic Editor: Fethi Bedioui

Received: 9 December 2021
Accepted: 29 December 2021
Published: 31 December 2021

1. Introduction

Gas sensors are of great interest due to their numerous applications and the possibility for a real-time analysis of several analytes [1–3]. Among these, resistive gas sensors exhibit attractive advantages compared with other gas sensors, such as fast and accurate gas detection, flexibility, low cost and small size [4]. The development of high-performance resistive gas sensors requires suitable gas-sensing materials in terms of both physical and chemical properties, such as morphology, crystalline structure, specific surface area and active sites. Since, as is well known, these characteristics all affect the performance of gas sensors, exploring and developing innovative materials has received attention in scientific research in recent years [5]. Attention is concentrated on the development of nanostructured materials, endowed with better sensing properties if compared to the same bulk material, such as carbon-based materials (in the form of carbon dots, nanotubes and graphene) [6–9], polymeric fibers (hybrid nanofibers) [10,11] and metal oxides semiconductor (MOS, as nanospheres, nanowires and nanosheets) [12–17]. Indeed, the large surface areas of nanomaterials ensure more active sites, enabling fast charge transfers and efficient gas-sensitive reactions [4].

Due to their widespread use in a variety of applications, in the recent years time-consuming, complex, and expensive traditional techniques have been substituted by these types of sensors. It has been especially evident in the field of volatile organic compound (VOC) detection, where traditional techniques, such as chromatography-mass spectrometry [18–21], generally lack ease of use, need specialized personnel and elaborate protocols,

and are characterized by high cost of the devices and insufficient flexibility. When early warning and quality monitoring applications are requested, resistive sensors are valuable alternatives. Indeed, in some specific applications, VOCs, such as diacetyl, need to be continuously monitored [22]. During the alcoholic fermentation processes of wine, beer and distilled beverages, diacetyl is naturally produced in small quantities, and it confers a characteristic butter-like aroma [23–27]. However, high diacetyl concentration (>5 mg/L) imparts an undesirable flavor indicating an alteration in the production or storage process. The time-monitoring of diacetyl concentrations can contribute to identifying and characterizing the quality of products [22]. Moreover, during this process, the so-called alcoholic fermentation, carbon dioxide and ethanol are produced too, and the influence of the atmosphere composition was reported to be fundamental in diacetyl detection and monitoring [28]. Till now, few works reported the detection of gaseous diacetyl mainly by means of complex array sensors [27,29,30]. Itoh et al. used variously-doped SnO_2 and CeO_2 to detect diacetyl among other volatile compounds [27], whereas PPy–V_2O_5 and PPy–ZnO nanocomposite fibers were successfully used by Pirsa et al. to discriminate the presence of diacetyl in fermented products [29]. Bailey et al. used an array of conducting polymers mounted on an electronic chip to discriminate between beers and to recognize the presence of volatile compounds, such as diacetyl [30].

In this work, tin oxide (SnO_2) is used to develop a high-performance resistive MOS sensor for the detection of VOCs [17,31], diacetyl in particular, thanks to the peculiar electrical properties of its microsphere structure [13]. The detection of diacetyl is performed by sampling the head space above the liquid solutions at different diacetyl concentrations (0.2–3.2 mg/L). The sensor has been tested using both aqueous and alcoholic (5% ethanol) diacetyl solutions in different carrier/regeneration gases, able to reproduce the typical alcoholic fermentation environment, rich in carbon dioxide (CO_2) and poor of oxygen. The revealed performance shows the promising ability of the of SnO_2 sensor to discriminate between different diacetyl concentrations in anaerobic atmospheres and in the contemporary presence of ethanol, generally characterized by a strong signal, identified as the major constituent of the headspace of alcoholic beverages [32]. Response and recovery time are also considered for a better investigation.

2. Materials and Methods

2.1. Tin Oxide Preparation and Charactetrization

A facile hydrothermal procedure was used to prepare SnO_2 powder, as reported elsewhere [13]. In detail, $SnCl_2$(II), used as the tin oxide precursor, was solubilized in ethanol (7.57 g/L). In order to fully dissolve $SnCl_2$, the mixture was firstly sonicated for 20 min and then it was transferred into a Teflon-lined stainless-steel autoclave at 200 °C for 6 h and 40 min. The solution was finally cooled down to room temperature. The obtained yellow solid was collected by centrifugation and washed in ethanol until the total removal of chloride ions. After ethanol washing the sample was dried at 80 °C overnight. The sample preparation procedure is schematically depicted in Figure 1.

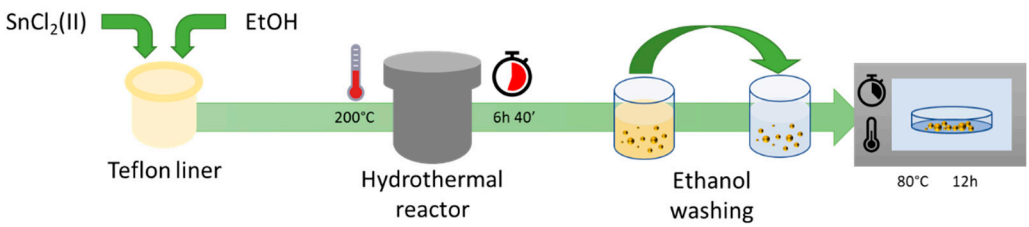

Figure 1. Synthesis procedure of SnO_2 metal oxide.

The sample was investigated using X-ray diffraction (XRD) analysis in the 2θ range from 10° to 65° (Cu Kα λ = 1.54056 Å) using steps of 0.02° and a count time of 5 s per step, with a temperature effect evaluation within 25–500 °C by using a PANalytical Empyrean

diffractometer equipped with an Anton Paar heat chamber. Peaks were attributed in accordance with the Crystallography Open Database (COD). The microstructure's morphology was studied by scanning electron microscopy, SEM, (Phenom Pro X).

2.2. Sensor Preparation and Testing

The sensing film was realized using a tin oxide/ethanol mixture sonicated for 15 min, in order to obtain a homogeneous paste, and deposited on an alumina planar substrate (6 mm × 3 mm) supplied with interdigitated Pt electrodes on the front side and a heating element on the back side [33]. The paste was dried at room temperature and finally annealed at 80 °C for 1 h. Before measurements, in order to improve the deposited film stability, the sensor was conditioned in air at 400 °C for 2 h. Tests were performed by positioning the sensor in a testing cell and flowing a total gas stream of 100 sccm. To assess the different working conditions' effects on the performance of the SnO_2 sensor, different pure gas atmospheres, namely Air, N_2 and CO_2 were evaluated. Diacetyl was chosen as the target analyte, both in aqueous and in alcoholic (5% ethanol) solutions. Analyte vapor was obtained by bubbling carrier gases in the solution that was maintained at 20 °C during the tests. All gas fluxes were measured by computer-controlled mass flow meters, and humidity was monitored and controlled to oscillate between 5% and 10%. The sensors' resistance data were collected in four-point mode by an Agilent 34970A (Santa Clara, CA, USA) multimeter, while sensor temperature was controlled by using a dual-channel power supplier instrument (Agilent E3632A, Santa Clara, CA, USA).

The sensor working temperature was fixed at 200 °C. Sensor response was defined as R/R_0 when the sensor showed an n-type response and the sensor resistance R measured in the presence of the reducing analyte gas decreased in respect to the sensor resistance R_0 of the sensor exposed to the carrier flow. Differently, when the sensor showed a p-type response and the sensor resistance R in the presence of the same analyte gas increased, the response was defined as R_0/R [34]. The response and recovery time of the sensor were defined as the time needed for the sensor to reach 90% of its saturation limit after the exposure to the analyte gas and as the time needed for the sensor to reach the 10% of its original resistance value once the target gas was switched off and the sensor was exposed to the carrier gas only, respectively [14].

3. Results and Discussion

3.1. SnO_2 Powder Characterization

The crystalline microstructure of the prepared SnO_2 was studied by XRD analysis, as shown in Figure 2a. The main characteristic peaks are centered at 26.7°, 34.2°, 37.8°, and 51.9° and correspond to the (110), (101), (200), and (211) SnO_2 crystal planes, respectively. The peaks appeared broad and with weak intensity, thus resulting with small average crystallite size and low crystallinity. This latter one was ascribed to the presence of defects on the material surface, which greatly affect the reactive sensing sites and electronic structure of gas-sensing material, influencing the gas sensing properties [35]. XRD spectra acquired at increasing temperatures, from 25 °C up to 500 °C, proved the high stability of the sample, being all the registered patterns superimposable.

The morphology of the powder was studied by SEM analysis. Figure 2b shows that sample is composed of homogeneous small particles of spherical form with size distribution ranging from 0.8 to 2.1 μm. A compact oxide thin film was used as the sensing layer.

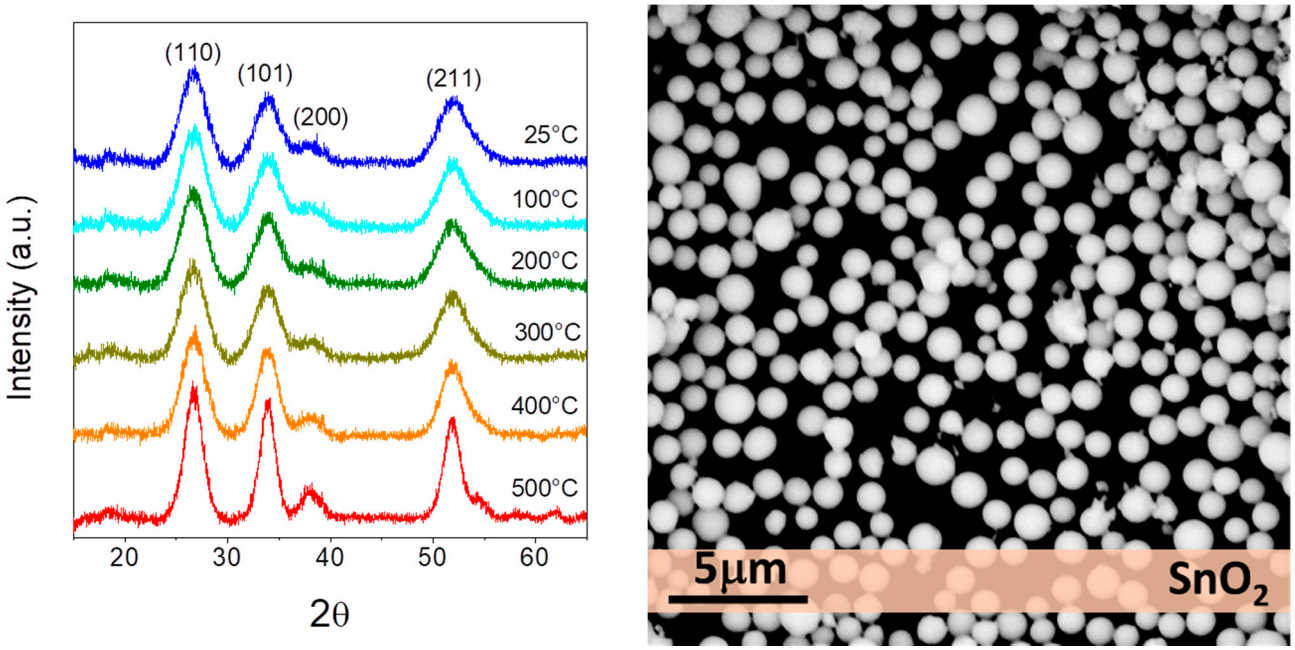

Figure 2. (**a**) XRD diffractograms versus temperatures and (**b**) SEM image of SnO_2 synthesized sample.

3.2. Gas Sensor Measurements

First, to study the behavior of the tin oxide sensor in different working atmospheres, the sensing properties toward vapors of diacetyl in aqueous solution (0.4 mg/L) were tested in oxidant, inert and reducing atmospheres, using as carrier and regeneration flow air N_2 and CO_2.

Tin oxide is well known as an MOS whose behavior is n-type. Indeed, the electrical resistance of the layer decrease when the sensor is exposed to reducing gas such as NH_3 [36], CO [37], CH_4 [38], H_2S [39] or SO_2 [40] due to the oxidation of the target gas on the SnO_2 surface. Measurements carried out under air and N_2 atmospheres (Figure 3a), confirmed the n-type behavior of the SnO_2 sensor with $R < R_0$, whereas the measurement carried out in CO_2 ambient showed an inverse behavior, with $R > R_0$, proving indeed that in CO_2, tin oxide worked as a p-type sensor.

3.2.1. Sensor Response in Air Atmosphere

SnO_2 response in air was widely studied and reported in literature [14]. Generally, in air the surface of SnO_2 is covered with negatively charged oxygen adsorbates (O_2^-, O^-, and O^{2-}). The formation of such oxygen adsorbates extracts electrons from the conduction band of SnO_2, bulk forming an electron depletion layer on the SnO_2 grains surface (space-charge region) and a potential barrier at the grain boundaries (Figure 3b) [41]; the sensor has a high resistance value (~30 MΩ). As soon as the sensor interacts with the analyte vapor, the diacetyl molecules are oxidized by oxygen species on the surface and the depleted layer electrons are fed back into SnO_2 bulk, thus a narrowed depletion layer and a reduction of the space-charge region is detected. Therefore, the sensor resistance decrease. In this case, exposing the sensor to 0.4 mg/L diacetyl solution vapors, the sensor response is equal to 1.43 and it results faster in the first seconds after the exposure, with a total response time of 3.0 min. Despite a very fast response being first observed, a delay in the sensor signal rise is detected; it demands a longer time to reach the final value. Indeed, the recording of the dynamic behavior of a sensor can be confusing, because the measured change in signal depends both on the intrinsic reaction of the gas sensing mechanism and

on a delayed change in test gas concentration [42]. Moreover, it should be highlighted that response/recovery times may be dependent on the measurement procedure.

On the contrary the recovery time is constant and slow (10.2 min).

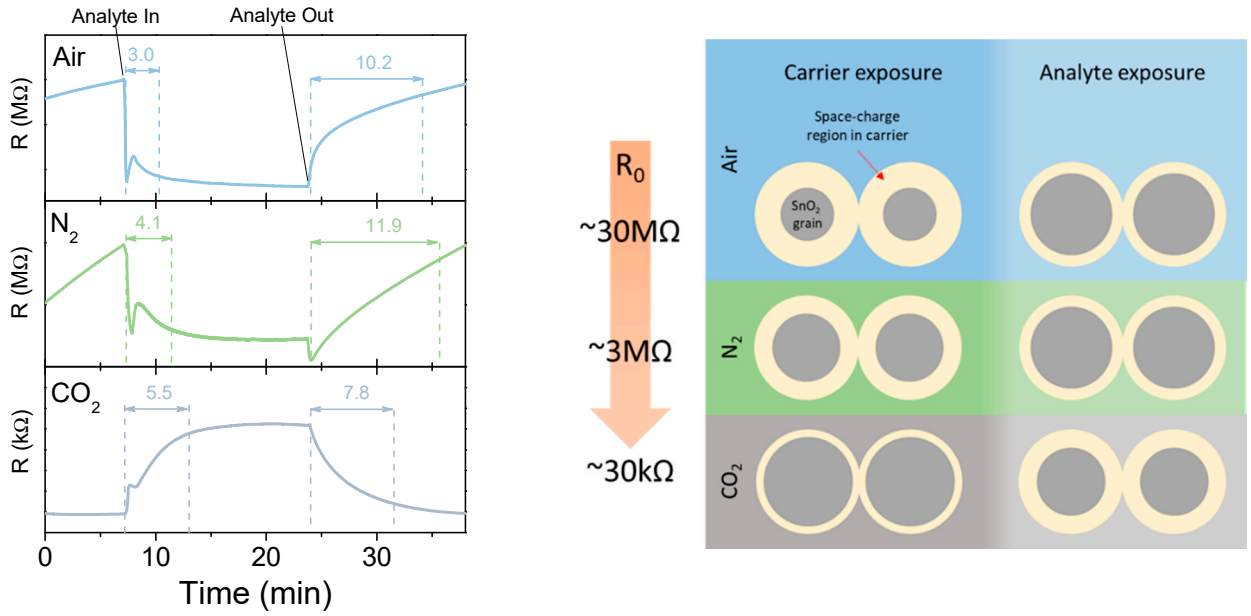

(**a**) (**b**)

Figure 3. Sensor measurements acquired in different atmospheres: (**a**) transient sensor response of 0.4 mg/L diacetyl in aqueous solution in air, N_2 and CO_2 environments; (**b**) schematic illustration of the sensing mechanism of SnO_2 powder to diacetyl in carrier and analyte exposure.

3.2.2. Sensor Response in N_2 Atmosphere

Under N_2 atmosphere the sensor showed a lower baseline resistance than in air (~3 MΩ). This result is compatible with the reduction of the density of oxygen species bound to the surface and then the increment of free carrier electrons into the conduction band that reduce the space-charge region at SnO_2 grains boundaries. The response to 0.4 mg/L diacetyl exposure confirms a typical n-type sensing, with a resistance decrement due to the interaction of diacetyl molecules with the surface. In addition, sensors tested under N_2 conditions shows a response comparable in terms of shape and magnitude with that observed under air, even if the sensor in N_2 atmosphere do not show a complete recovery. A similar trend was already observed with a SnO_2 sensor in argon atmosphere [43]. Measurements performed in air and N_2 appeared with the same shape. Previews works indicated that despite a traditional n-type response was observed, in absence of oxygen the sensing mechanism is related to the direct adsorption of VOC on the MOS surface [43].

The sensor response in N_2 is 1.60, but both response and recovery time result longer than in air measurements cause the poor interaction between N_2 carrier and the sensor surface.

3.2.3. Sensor Response in CO_2 Atmosphere

In a pure-CO_2 atmosphere the resistance R is greater than R_0, revealing a p-type behavior. In this condition the sensor is able to detect diacetyl and shows a total recovery in short time.

In a CO_2 atmosphere R resulted smaller than both in air and N_2 (~30 kΩ). Indeed, according to Wang et al., when SnO_2 works at 240 °C in high CO_2 concentrations and less than 14% relative humidity conditions, CO_2 acts as an electron donor, as a weak reducing agent [14]. Such a response-type transition is also observed for other materials,

and it is due to the inversion of the conduction type of major carriers, which limits the dynamic range of the sensor at high concentration [44]. In the pure-CO_2 atmosphere the sensor response to 0.4 mg/L diacetyl exposure is 1.13, with response and recovery times of 5.5 min and 7.8 min, respectively. Recovery time results are shorter than in air and in N_2 atmosphere cases.

3.2.4. Sensor Response towards Diacetyl in Aqueous and Alcholic Solutions

Once the effect of the different carrier/regeneration atmospheres on the performance of SnO_2 towards diacetyl was evaluated, just oxygen-deficient atmospheres were considered. Indeed, alcoholic fermentation, producing ethanol and carbon dioxide, usually occurs in anaerobic environments, since it does not require oxygen. Hence, tests were further performed in oxygen-deficient atmospheres, N_2 and CO_2, in: (i) aqueous diacetyl solution (0.4 mg/L); (ii) alcoholic (5% ethanol) diacetyl solution (0.4 mg/L), and (iii) alcoholic (5% ethanol) solution, for comparison purposes. The response values along with the response and recovery time are summarized in Figure 4.

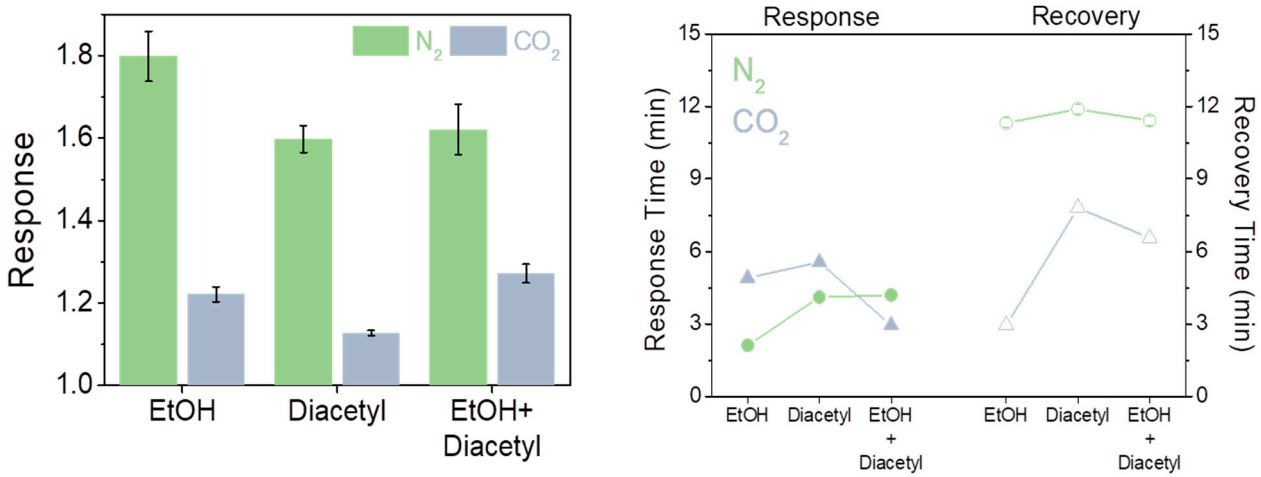

(**a**) (**b**)

Figure 4. (**a**) Sensor response in N_2 and CO_2 to alcoholic (5% ethanol) solution, aqueous diacetyl solution (0.4 mg/L) and alcoholic (5% ethanol) diacetyl solution (0.4 mg/L). Error bars are calculated on three runs; (**b**) response and recovery times of sensor exposed at different concentration of diacetyl in aqueous and alcoholic solutions in CO_2 and N_2 ambient. Error bars are calculated on three runs.

The sensor in both N_2 and CO_2 environments shows a higher response to ethanol than diacetyl, reaching 1.80 and 1.22, respectively, with shorter response and recovery times. In alcoholic diacetyl solution, the response in N_2 ambient registers a value of 1.61, similar to the value found with the only-diacetyl solution, and response and recovery time results are similar, showing that under N_2 atmosphere it is very difficult to distinguish diacetyl effects in aqueous or alcoholic solutions. Instead, in a CO_2 atmosphere an increment in the response towards diacetyl alcoholic solution, with a final value of 1.27, is detected. In turns, the sensor, despite the lower response than in CO_2, succeeds in distinguishing diacetyl under fermentation conditions. Moreover, response time in CO_2 shows a marked decrement (46%) compared to only diacetyl. Similarly, recovery time is reduced too.

3.2.5. Effect of Diacetyl Concentrations in Alcholic and Aqueous Solutions

The fabricated SnO_2 sensor was investigated by varying the diacetyl concentration both in aqueous and alcoholic solutions in a CO_2 environment (Figure 5). The response curves for different diacetyl concentrations (0.05–3.2 mg/L) are reported in Figure 5a,b. It can be seen that the response of the SnO_2 sensor increases by increasing diacetyl concentration with an exponential trend. The response of the sensor (Y) can be fitted as a

logarithmic function of Y = 1.14 + 0.07logX with X representing the diacetyl concentration in mg/L and with a regression coefficient R^2 of 0.97, as shown in the inset of Figure 5a. An exponential trend of the response depending on the diacetyl concentration in alcoholic solution is instead reported in Figure 5b. The sensor response in the alcoholic solution results higher than diacetyl in a water solution, following a logarithm profile. This is due to the high sensitivity of SnO_2 to ethanol as reported in previous works [37,38]. Moreover, the presence of ethanol markedly enhanced the gas sensing performance toward diacetyl in the alcoholic solution.

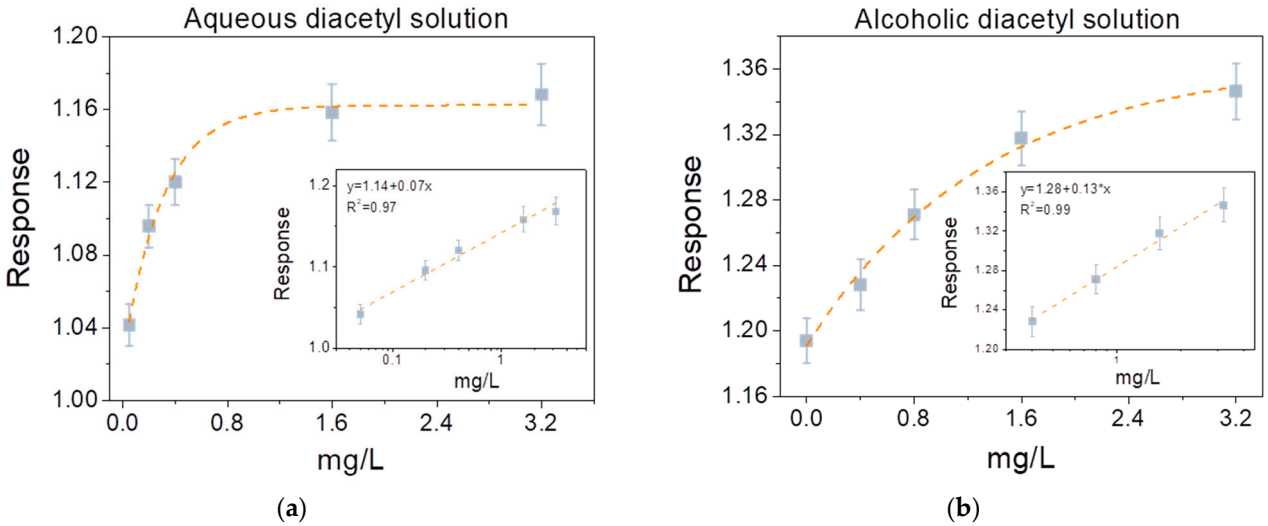

Figure 5. Sensor response in CO_2 atmospheres at different diacetyl concentrations in (**a**) aqueous solution and (**b**) alcoholic solution. Error bars are calculated on three runs.

By fitting the sensor response with a logarithmic function Y = 1.28 + 0.13logX (R^2 = 0.99) it is evident how the slope of the curve is greater than the response of diacetyl in water solution. From the fit it is possible to extract the lower detection limit (LDL), the minimum concentration of gas detectable by gas sensor [45,46].

For SnO_2 sensor LDL can be estimated by the extrapolation of the linear fit of the response curve down to the minimum response R_{min}/R_0 where $R_{min} = R_0 - 3\sigma$, and σ is the standard deviation of the baseline resistance before analyte exposure. For diacetyl in an aqueous solution LDL results 0.1 mg/L, while for measurements performed on diacetyl in an alcoholic solution LDL is less than 0.01 mg/L. In turn, ethanol presence increases the sensitivity of the sensor, proving the capability of the SnO_2 sensor to detect diacetyl in alcoholic solution in a CO_2 atmosphere.

3.2.6. Response and Recovery Time in Alcholic Diacetyl Solution

Response and recovery times of diacetyl in alcoholic solution under a CO_2 atmosphere are analyzed, being important to understand the performance of the sensor.

Figure 6a shows response/recovery times of the SnO_2 sensor in different diacetyl concentrations. Their analysis shows that for all the evaluated diacetyl concentrations, recovery time is higher than response time. Response and recovery time values decrease with an exponential law upon increasing the concentration; response time is almost halved, from 3.2 min to 1.7 min with a diacetyl increment from 0.4 mg/L to 3.2 mg/L. Analogously, the recovery time decreases from 6.6 min to 2.2 min in the same working conditions. According to literature data [42], basic effects of surface covering kinetics and diffusion may be the cause of a dependence on concentration change. Moreover, since the semiconductor can be considered as an RC filter with a time constant τ, electronic effects may have influence too. Due to the increasing of diacetyl concentration, the resistance decreases and thus also the time constant.

Indeed, the sensor resistance as a function of time during the exposure to the analyte and during the recovery can be described through the following equations [42]:

$$R(t) = R_{max} - (R_{max} - R_0) \exp\left[\frac{-t}{\tau_{resp}}\right], \quad (1)$$

$$R(t) = R_0 + (R_{max} - R_0) \exp\left[\frac{-t}{\tau_{rec}}\right], \quad (2)$$

where R(t) is the resistance after the analyte exposure, R_0 is a constant, R_{max} is the saturated resistance, t is the time, and τ_{resp} and τ_{rec} are the response and recovery time constants, respectively. Figure 6b shows the plot of time constants as a function of diacetyl concentration. The curves show that the time constants decreased as diacetyl concentration increased. According to response and recovery time analysis, the range of τ values recorded at low diacetyl concentration is much wider than that recorded at high diacetyl concentration, where τ is less than 50 s.

The parameter τ is therefore considered a more suitable parameter to characterize sensors response and recovery times.

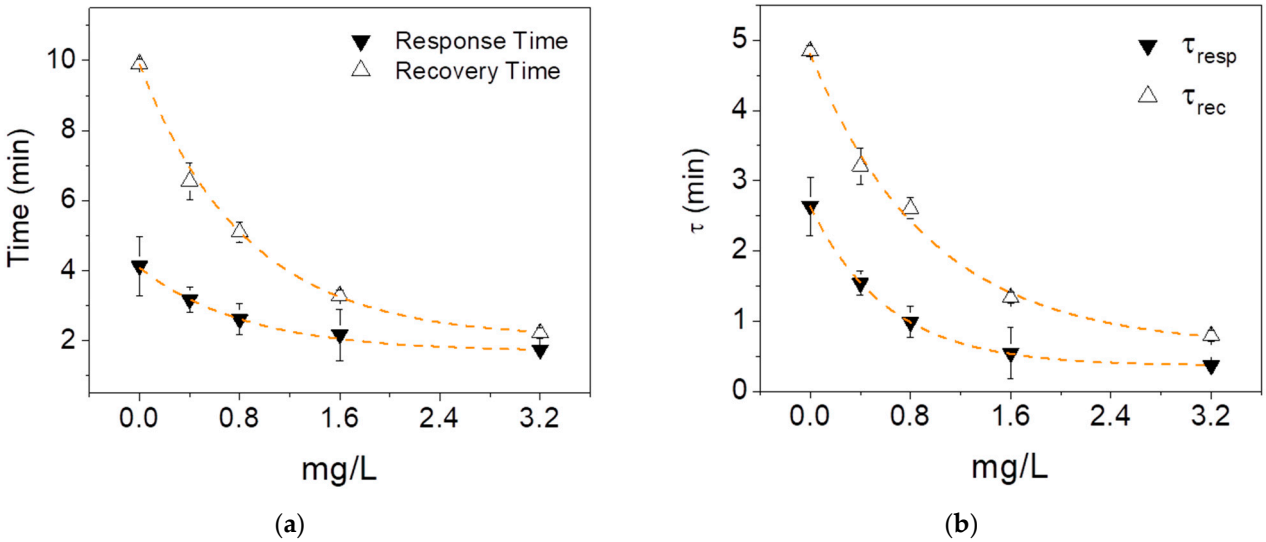

(**a**) (**b**)

Figure 6. Time parameters for sensor exposed at different concentration of diacetyl in alcoholic solution and a CO_2 environment; (**a**) sensor response and recovery times at different diacetyl concentration; (**b**) plot of time constants as a function of diacetyl concentration. Error bars are calculated on three runs.

4. Conclusions

A SnO_2-based MOS sensor is used to investigate the detection of VOCs in fermented beverages such as beer, wine and distillates. Synthesized and characterized SnO_2 is used to discriminate the concentration of diacetyl vapors in different operating atmospheres, as to replicate a typical alcoholic fermentation scenario.

Under air, N_2 and CO_2 gases, SnO_2 shows different behavior and baseline resistances due to different interactions with its surface. In particular, measurements carried out under air and N_2 atmospheres show the n-type behavior of the SnO_2 sensor, whereas measurements carried out in CO_2 ambient prove that SnO_2 acted as a p-type sensor.

Tests performed in aqueous and alcoholic diacetyl solutions show good response in terms of diacetyl detection in the range of concentration 0.2–3.2 mg/L at 200 °C in CO_2 atmosphere, with LDL of 0.1 mg/L and 0.01 mg/L, respectively.

Response and recovery times trends reveal the diacetyl concentration dependance, with response and recovery times constant less than 50 s.

Author Contributions: Conceptualization, A.G., A.F., L.B. and A.D.; methodology, A.G., A.F. and L.B.; formal analysis, A.G. and A.F.; investigation, A.G. and A.F.; data curation, A.G.; writing—original draft preparation, A.G. and A.F.; writing—review and editing, A.G. and L.B.; supervision L.B. and A.D. All authors have read and agreed to the published version of the manuscript.

Funding: This research was co-financed with the support of the European Commission, the European Social Fund and the Calabria Region. The author is solely responsible for this research and the European Commission and the Calabria Region decline any responsibility for the use that may be made of the information contained therein.

Institutional Review Board Statement: Not applicable.

Conflicts of Interest: The authors declare no conflict of interest.

References

1. Wu, H.; Shi, L. Real-time anomaly detection in gas sensor streaming data. *Int. J. Embed. Syst.* **2021**, *14*, 81–88. [CrossRef]
2. Nazemi, H.; Joseph, A.; Park, J.; Emadi, A. Advanced Micro- and Nano-Gas Sensor Technology: A Review. *Sensors* **2019**, *19*, 1285. [CrossRef]
3. Malara, A.; Bonaccorsi, L.; Donato, A.; Frontera, P.; Neri, G. Doped Zinc Oxide Sensors for Hexanal Detection. In *Lecture Notes in Electrical Engineering*; Springer: Singapore, 2020; pp. 279–285.
4. Wang, Z.; Zhu, L.; Sun, S.; Wang, J.; Yan, W. One-Dimensional Nanomaterials in Resistive Gas Sensor: From Material Design to Application. *Chemosensors* **2021**, *9*, 198. [CrossRef]
5. Zhou, X.; Lee, S.; Xu, Z.; Yoon, J. Recent Progress on the Development of Chemosensors for Gases. *Chem. Rev.* **2015**, *115*, 7944–8000. [CrossRef] [PubMed]
6. Faggio, G.; Gnisci, A.; Messina, G.D.S.; Lisi, N.; Capasso, A.; Lee, G.-H.; Armano, A.; Sciortino, A.; Messina, F.; Cannas, M.; et al. Carbon Dots Dispersed on Graphene/SiO2/Si: A Morphological Study. *Phys. Status Solidi* **2019**, *216*, 1800559. [CrossRef]
7. Sawalha, S.; Moulaee, K.; Nocito, G.; Silvestri, A.; Petralia, S.; Prato, M.; Bettini, S.; Valli, L.; Conoci, S.; Neri, G. Carbon-dots conductometric sensor for high performance gas sensing. *Carbon Trends* **2021**, *5*, 100105. [CrossRef]
8. Malara, A.; Leonardi, S.G.; Bonavita, A.; Fazio, E.; Stelitano, S.; Neri, G.; Neri, F.; Santangelo, S. Origin of the different behavior of some platinum decorated nanocarbons towards the electrochemical oxidation of hydrogen peroxide. *Mater. Chem. Phys.* **2016**, *184*, 269–278. [CrossRef]
9. Nag, A.; Mitra, A.; Mukhopadhyay, S. Graphene and its sensor-based applications: A review. *Sens. Actuators A Phys.* **2018**, *270*, 177–194. [CrossRef]
10. Busacca, C.; Donato, A.; Faro, M.L.; Malara, A.; Neri, G.; Trocino, S. CO gas sensing performance of electrospun Co_3O_4 nanostructures at low operating temperature. *Sens. Actuators B Chem.* **2020**, *303*, 127193. [CrossRef]
11. Kailasa, S.; Reddy, M.S.B.; Maurya, M.R.; Rani, B.G.; Rao, K.V.; Sadasivuni, K.K. Electrospun Nanofibers: Materials, Synthesis Parameters, and Their Role in Sensing Applications. *Macromol. Mater. Eng.* **2021**, *306*, 2100410. [CrossRef]
12. Radhakrishnan, J.; Kumara, M. Geetika Effect of temperature modulation, on the gas sensing characteristics of ZnO nanostructures, for gases O_2, CO and CO_2. *Sens. Int.* **2021**, *2*, 100059. [CrossRef]
13. Zhang, L.; Tong, R.; Ge, W.; Guo, R.; Shirsath, S.E.; Zhu, J. Facile one-step hydrothermal synthesis of SnO_2 microspheres with oxygen vacancies for superior ethanol sensor. *J. Alloys Compd.* **2020**, *814*, 152266. [CrossRef]
14. Wang, D.; Chen, Y.; Liu, Z.; Li, L.; Shi, C.; Qin, H.; Hu, J. CO2-sensing properties and mechanism of nano-SnO_2 thick-film sensor. *Sens. Actuators B Chem.* **2016**, *227*, 73–84. [CrossRef]
15. Hoa, T.T.N.; Van Duy, N.; Hung, C.M.; Van Hieu, N.; Hau, H.H.; Hoa, N.D. Dip-coating decoration of Ag_2O nanoparticles on SnO_2 nanowires for high-performance H2S gas sensors. *RSC Adv.* **2020**, *10*, 17713–17723. [CrossRef]
16. Sun, P.; Mei, X.; Cai, Y.; Ma, J.; Sun, Y.; Liang, X.; Liu, F.; Lu, G. Synthesis and gas sensing properties of hierarchical SnO_2 nanostructures. *Sens. Actuators B Chem.* **2013**, *187*, 301–307. [CrossRef]
17. Gnisci, A.; Fotia, A.; Malara, A.; Bonaccorsi, L.; Frontera, P.; Donato, A. SnO_2 sensing performance toward volatile organic compounds. In Proceedings of the CSAC2021: 1st International Electronic Conference on Chemical Sensors and Analytical Chemistry, Online, 1–15 July 2021; Malara, A., Ed.; MDPI: Basel, Switzerland, 2021.
18. Parish, M.E.; Braddock, R.J.; Wicker, L. Gas Chromatographic Detection of Diacetyl in Orange Juice. *J. Food Qual.* **1990**, *13*, 249–258. [CrossRef]
19. Macciola, V.; Candela, G.; De Leonardis, A. Rapid gas-chromatographic method for the determination of diacetyl in milk, fermented milk and butter. *Food Control.* **2008**, *19*, 873–878. [CrossRef]
20. Otsuka, M.; Ohmori, S. Simple and sensitive determination of diacetyl and acetoin in biological samples and alcoholic drinks by gas chromatography with electron-capture detection. *J. Chromatogr. B Biomed. Sci. Appl.* **1992**, *577*, 215–220. [CrossRef]
21. Tian, J. Determination of several flavours in beer with headspace sampling–gas chromatography. *Food Chem.* **2010**, *123*, 1318–1321. [CrossRef]
22. Clark, S.; Winter, C.K. Diacetyl in Foods: A Review of Safety and Sensory Characteristics. *Compr. Rev. Food Sci. Food Saf.* **2015**, *14*, 634–643. [CrossRef]

23. Li, P.; Guo, X.; Shi, T.; Hu, Z.; Chen, Y.; Du, L.; Xiao, D. Reducing diacetyl production of wine by overexpressing BDH1 and BDH2 in Saccharomyces uvarum. *J. Ind. Microbiol. Biotechnol.* **2017**, *44*, 1541–1550. [CrossRef]
24. Martineau, B.; Acree, T.E.; Henick-Kling, T. Effect of wine type on the detection threshold for diacetyl. *Food Res. Int.* **1995**, *28*, 139–143. [CrossRef]
25. Krogerus, K.; Gibson, B.R. 125thAnniversary Review: Diacetyl and its control during brewery fermentation. *J. Inst. Brew.* **2013**, *119*, 86–97. [CrossRef]
26. Lee, H.-H.; Lee, K.-T.; Shin, J.-A. Analytical method validation and monitoring of diacetyl in liquors from Korean market. *Food Sci. Biotechnol.* **2017**, *26*, 893–899. [CrossRef] [PubMed]
27. Itoh, T.; Koyama, Y.; Shin, W.; Akamatsu, T.; Tsuruta, A.; Masuda, Y.; Uchiyama, K. Selective Detection of Target Volatile Organic Compounds in Contaminated Air Using Sensor Array with Machine Learning: Aging Notes and Mold Smells in Simulated Automobile Interior Contaminant Gases. *Sensors* **2020**, *20*, 2687. [CrossRef] [PubMed]
28. Portno, A.D. The influence of oxygen on the production of diacetyl during fermentation and conditioning. *J. Inst. Brew.* **1966**, *72*, 458–461. [CrossRef]
29. Pirsa, S.; Nejad, F.M. Simultaneous analysis of some volatile compounds in food samples by array gas sensors based on polypyrrole nano-composites. *Sens. Rev.* **2017**, *37*, 155–164. [CrossRef]
30. Bailey, T.P.; Hammond, R.V.; Persaud, K.C. Applications for an Electronic Aroma Detector in the Analysis of Beer and Raw Materials. *J. Am. Soc. Brew. Chem.* **1995**, *53*, 39–42. [CrossRef]
31. Malara, A.; Bonaccorsi, L.; Donato, A.; Frontera, P.; Piscopo, A.; Poiana, M.; Leonardi, S.G.; Neri, G. Sensing Properties of Indium, Tin and Zinc Oxides for Hexanal Detection. In *Lecture Notes in Electrical Engineering*; Springer: Singapore, 2019; pp. 39–44.
32. Ragazzo-Sanchez, J.A.; Chalier, P.; Chevalier, D.; Ghommidh, C. Electronic nose discrimination of aroma compounds in alcoholised solutions. *Sens. Actuators B Chem.* **2006**, *114*, 665–673. [CrossRef]
33. Bonaccorsi, L.; Malara, A.; Donato, A.; Donato, N.; Leonardi, S.G.; Neri, G. Effects of UV Irradiation on the Sensing Properties of In2O3 for CO Detection at Low Temperature. *Micromachines* **2019**, *10*, 338. [CrossRef]
34. Williams, D.E. Semiconducting oxides as gas-sensitive resistors. *Sens. Actuators B Chem.* **1999**, *57*, 1–16. [CrossRef]
35. Liu, L.; Shu, S.; Zhang, G.; Liu, S. Highly Selective Sensing of C2H6O, HCHO, and C3H6O Gases by Controlling SnO_2 Nanoparticle Vacancies. *ACS Appl. Nano Mater.* **2018**, *1*, 31–37. [CrossRef]
36. Shahabuddin, M.; Sharma, A.; Kumar, J.; Tomar, M.; Umar, A.; Gupta, V. Metal clusters activated SnO_2 thin film for low level detection of NH3 gas. *Sens. Actuators B Chem.* **2014**, *194*, 410–418. [CrossRef]
37. Hermida, I.D.P.; Wiranto, G.; Hiskia; Nopriyanti, R. Fabrication of SnO_2based CO gas sensor device using thick film technology. *J. Phys. Conf. Ser.* **2016**, *776*, 012061. [CrossRef]
38. Sedghi, S.M.; Mortazavi, Y.; Khodadadi, A.A. Low temperature CO and CH4 dual selective gas sensor using SnO_2 quantum dots prepared by sonochemical method. *Sens. Actuators B Chem.* **2010**, *145*, 7–12. [CrossRef]
39. Devi, G.S.; Manorama, S.; Rao, V. High sensitivity and selectivity of an SnO_2 sensor to H2S at around 100 °C. *Sens. Actuators B Chem.* **1995**, *28*, 31–37. [CrossRef]
40. Das, S.; Girija, K.; Debnath, A.; Vatsa, R. Enhanced NO_2 and SO_2 sensor response under ambient conditions by polyol synthesized Ni doped SnO_2 nanoparticles. *J. Alloys Compd.* **2021**, *854*, 157276. [CrossRef]
41. Shimizu, Y. *SnO_2 Gas Sensor BT—Encyclopedia of Applied Electrochemistry*; Kreysa, G., Ota, K., Savinell, R.F., Eds.; Springer: New York, NY, USA, 2014; pp. 1974–1982. ISBN 978-1-4419-6996-5.
42. Hübert, T.; Majewski, J.; Banach, U.; Detjens, M.; Tiebe, C. Response Time Measurement of Hydrogen Sensors. 2017. Available online: https://hysafe.info/uploads/2017_papers/211.pdf (accessed on 28 December 2021).
43. Abokifa, A.A.; Haddad, K.; Fortner, J.; Lo, C.S.; Biswas, P. Sensing mechanism of ethanol and acetone at room temperature by SnO_2 nano-columns synthesized by aerosol routes: Theoretical calculations compared to experimental results. *J. Mater. Chem. A* **2018**, *6*, 2053–2066. [CrossRef]
44. Liu, X.-L.; Zhao, Y.; Ma, S.-X.; Zhu, S.-W.; Ning, X.-J.; Zhao, L.; Zhuang, J. Rapid and Wide-Range Detection of NOx Gas by N-Hyperdoped Silicon with the Assistance of a Photovoltaic Self-Powered Sensing Mode. *ACS Sens.* **2019**, *4*, 3056–3065. [CrossRef]
45. Barsan, N.; Weimar, U. Conduction Model of Metal Oxide Gas Sensors. *J. Electroceram.* **2001**, *7*, 143–167. [CrossRef]
46. Santos, G.T.; Felix, A.A.; Orlandi, M.O. Ultrafast Growth of h-MoO_3 Microrods and Its Acetone Sensing Performance. *Surfaces* **2021**, *4*, 9–16. [CrossRef]